EE

C.E. SACLAY
DSM

SERVICE D'ÉTUDE DES ACCÉLÉRATEURS

DAPNIA/SEA-96-06 06/1996

Spectral Analysis of Alignment Techniques for Linear Colliders

Andrey SERY and Alban MOSNIER

DAPNIA

Couverture : Sylvie Cabrit et Marc Sauvage

Le DAPNIA (**D**épartement d'**A**strophysique, de physique des **P**articules, de physique **N**ucléaire et de l'**I**nstrumentation **A**ssociée) regroupe les activités du Service d'Astrophysique (SAp), du Département de Physique des Particules Elémentaires (DPhPE) et du Département de Physique Nucléaire (DPhN).

Adresse : DAPNIA, Bâtiment 141
CEA Saclay
F - 91191 Gif-sur-Yvette Cedex

Submitted to Physical Review E

DAPNIA/SEA 96 06

SPECTRAL ANALYSIS OF ALIGNMENT TECHNIQUES FOR LINEAR COLLIDERS

Andrey SERY* and Alban MOSNIER
CEA, DSM/DAPNIA
CE-Saclay, F-91191 Gif-sur-Yvette Cedex, France

June 20, 1996

Abstract

Spectral analysis has been used to study emittance growth due to chromatic effects in future linear colliders. This formalism allows to study the effects of static initial misalignments, as well as the effects of magnet displacements produced by ground motion, the latter described adequately by the two dimensional power spectrum $P(\omega, k)$. The effectiveness of correction techniques, envisaged in long linacs to recover the small required emittance has been also evaluated by this spectral approach. For illustration, analytical predictions for the "one-to-one" algorithm and the "adaptive alignment" method are given and compared to numerical simulations.

*Permanent address: Branch of the Institute of Nuclear Physics, 142284 Protvino, Moscow region, Russia

1 Introduction

Ground motion is of major concern in future linear colliders because it will displace focusing magnets, which, in turn, will dilute the beam emittance in the linac through dispersive effects. Beam-based alignment techniques will recover either the proper alignment of the elements or the "gold" trajectory, which minimizes dispersion, nevertheless steering feedback loops are needed to control the chromatic dilution on a continuous-time basis against the ground motion. The beam-based alignment correction, which requires measurements of the beam orbit with different quadrupole settings, will be used periodically, with some rather long time intervals, while steering algorithms will be applied continuously in between.

In this paper, a spectral analysis is presented which evaluates the final dispersive error for initial misalignments, but also after alignment or trajectory correction techniques. Furthermore, this spectral approach makes use of the 2-dimensional power spectrum [1, 2], which gives a complete description of ground motion — including time and space dependence of displacements — and permits not only static (e.g. initial misalignment), but also dynamic study of the effectiveness of alignment algorithms. For illustration, the method is applied first to the so called "one-to-one" algorithm (see [3], for example), when simple steering dipoles are used or when quadrupole can be mechanically moved, second to the "adaptive alignment" method proposed by V. Balakin [4]. Analytical predictions giving the quadrupole spectra and the final dispersion are compared to numerical simulations. The limitations of the presented spectral approach are finally discussed.

2 Spectral analysis of chromatic dilution

Beam emittance growth, induced by chromatic effects, can be studied with the help of the spectral approach. When we consider static initial misalignments of focusing magnets, or displacements produced by ground motion, the chromatic dilution is simply given by an integral involving the power spectrum of the displacements and a spectral response function describing the transport line. We will show that this formalism can be extended also for the case when correction techniques become operative, provided that the correlation between space harmonics, which now arises, is correctly taken into account.

On the Fig.1, showing some focusing quadrupoles of a linac, $x_i(t) = x(t, s_i)$ is the transverse position of the i-th element, measured relatively to the reference line, a_i is the BPM reading, s_i is the longitudinal position $s_i = iL$, L is the quadrupole spacing. If $x_{\rm abs}(t, s)$ is the coordinate measured in an inertial frame and the reference line passes through the entrance, then the transverse position is $x(t, s) = x_{\rm abs}(t, s) - x_{\rm abs}(t, 0)$.

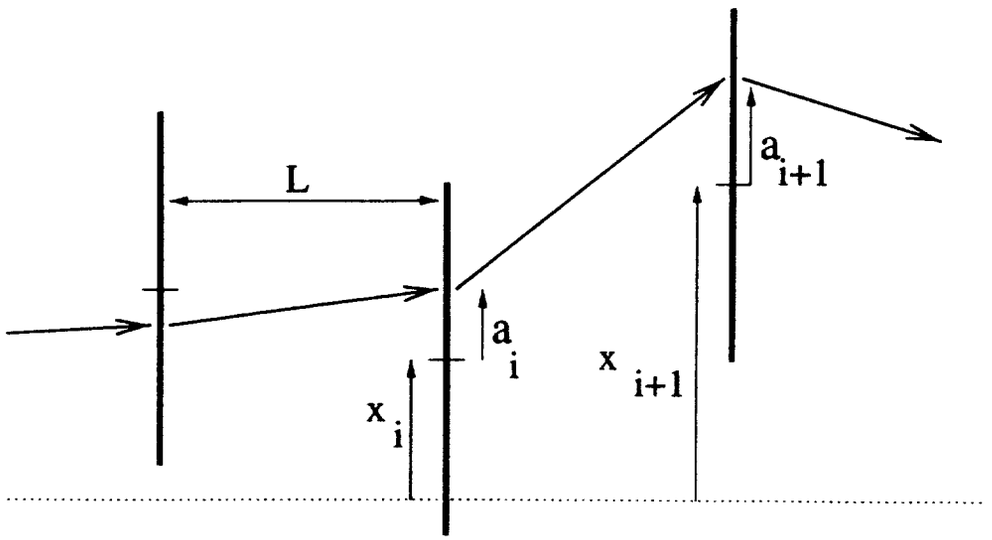

Figure 1: Misaligned quadrupoles. Here x_i is quadrupole displacement relative to the reference line, a_i is the BPM reading.

Dispersive errors arise because particles having different energies in the bunch are deflected differently by the misaligned quadrupoles. Although the offset at the exit $x^*(t)$ is not strictly a linear function of the relative energy deviation δ, we will consider henceforth only the linear term, defined as $\eta_x(t) = dx^*(t)/d\delta$, for the estimation of the chromatic dilution.

Let b_i and d_i be the first derivatives of the beam offset and of the beam dispersion at the exit of the linac with respect to the displacement of the element i. The final offset, measured relatively to the reference line, and dispersive error are given by the summation of all the deflections experienced by the beam

$$x^*(t) = R_{11}x_{\rm inj}(t) + R_{12}x'_{\rm inj}(t) + \sum_{i=1}^{N} b_i\, x_i(t) \tag{1}$$

$$\eta_x(t) = T_{116}x_{\rm inj}(t) + T_{126}x'_{\rm inj}(t) + \sum_{i=1}^{N} d_i\, x_i(t) \tag{2}$$

Here N is the total number of quadrupoles, the R and T are the first and second order total matrixes of the considered transport line. The values $x_{\rm inj}(t)$ and $x'_{\rm inj}(t)$ are the position and the angle of the injected beam at the entrance.

We assume that the beam is injected along the reference line. In practice it means that the beam is menaged to pass through the center of some element, say a beam position monitor, placed at the entrance, i.e. at $s = 0$. In this case $x_{\rm inj}(t) = 0$ and $x'_{\rm inj}(t) = 0$ and the formulae (1, 2) can be rewritten in this way

$$x^*(t) = \sum_{i=1}^{N} b_i\, x_i(t) \tag{3}$$

$$\eta_x(t) = \sum_{i=1}^{N} d_i\, x_i(t) \tag{4}$$

Assuming that the beam can be re-aligned at the exit, we will now focus on the final dispersion only. While the mean value of the dispersion $\langle \eta_x(t) \rangle$, averaged on realizations, is zero, the mean squared value gives the dispersive error:

$$\langle \eta_x^2(t) \rangle = \sum_i \sum_j d_i d_j \, \langle x_i(t) x_j(t) \rangle \tag{5}$$

The displacement $x(t,s)$ is a 2-dimensional function of time and position along the linac. One can introduce the spatial harmonics $x(t,k)$ of wave number $k = 2\pi/\lambda$, with λ the spatial period of displacements:

$$x(t,k) = \int_{-\mathcal{L}/2}^{\mathcal{L}/2} x(t,s) e^{-iks} ds \tag{6}$$

The function $x(t,k)$ is complex, with a symmetrical real part and an asymmetrical imaginary part, relative to $k = 0$. The displacement $x(t,s)$ can be written using the back transformation:

$$x(t,s) = \int_{-\infty}^{\infty} x(t,k)(e^{iks} - 1)\frac{dk}{2\pi} \tag{7}$$

which ensures that at the entrance $x(t, s = 0) = 0$. The dispersive error (5) can then be written

$$\langle \eta_x^2(t) \rangle = \sum_i \sum_j d_i d_j \int_{-\infty}^{\infty} \int_{-\infty}^{\infty} \langle x(t,k_1) x^*(t,k_2) \rangle (e^{ik_1 s_i} - 1)(e^{-ik_2 s_j} - 1) \frac{dk_1}{2\pi} \frac{dk_2}{2\pi} \tag{8}$$

This general form allows the eventual dependence of spatial harmonics. We first consider the case of initial misalignment or (and) ground motion, where all spatial harmonics are assumed to be independent. The dispersive error becomes

$$\langle \eta_x^2(t) \rangle = \sum_i \sum_j d_i d_j \int_{-\infty}^{\infty} P(t,k)(e^{iks_i} - 1)\,(e^{-iks_j} - 1)\frac{dk}{2\pi} \tag{9}$$

One can rewrite (9) in the way, which separate lattice properties and displacements properties

$$\langle \eta_x^2(t) \rangle = \int_{-\infty}^{\infty} P(t,k)\, G(k)\, \frac{dk}{2\pi} \tag{10}$$

Here $G(k)$ is the so called spectral response function of the considered transport line

$$G(k) = g_c^2(k) + g_s^2(k) \tag{11}$$

with

$$g_c(k) = \sum_{i=1}^{N} d_i(\cos(ks_i) - 1) \quad \text{and} \quad g_s(k) = \sum_{i=1}^{N} d_i \sin(ks_i) \tag{12}$$

The spatial power spectrum of displacements $x(t,s)$ is defined as

$$P(t,k) = \lim_{\mathcal{L}\to\infty} \frac{1}{\mathcal{L}} x(t,k)x^*(t,k) = \lim_{\mathcal{L}\to\infty} \frac{1}{\mathcal{L}} \left| \int_{-\mathcal{L}/2}^{\mathcal{L}/2} x(t,s)e^{-iks} ds \right|^2 \tag{13}$$

it is a real function.

The power spectrum of displacements $P(t,k)$ can be easily found as far as initial misalignment or ground motion are concerned. For example, assume that the focusing elements are perfectly aligned along the reference line at $t = 0$ and then are moved by ground motion. The evolution of the power spectrum can be described by the following expression [1, 2]:

$$P(t,k) = \int_{-\infty}^{\infty} P(\omega,k)\ 2[1 - \cos(\omega t)] \frac{d\omega}{2\pi} \tag{14}$$

where the two-dimensional power spectrum $P(\omega,k)$ characterizes ground motion properties, including both spatial and temporal correlation information. Several models of $P(\omega,k)$, based on measured data, have been proposed in [2]. The diffusive ground motion, leading to large displacements after long time intervals, is usually described by the "ATL law" [5]. Its power spectrum $P(\omega,k)$ is simply:

$$P(\omega,k) = \frac{A}{\omega^2 k^2} \tag{15}$$

A typical value of the coefficient A is $A = 10^{-5}\mu\text{m}^2\text{s}^{-1}\text{m}^{-1}$. Though any type of $P(\omega,k)$ can be considered, we will keep only this particular motion for the estimation of the dispersion throughout this paper.

When correction procedures interfere, spatial harmonics can be not any more independent and correlation of phases between two harmonics with different wave numbers can arise. In principle, the phase of a given k-th harmonics may be linked to all other harmonics. This correlation, which is lost through the power spectrum $P(t,k)$, may change the result significantly. Therefore one have to use expression (8) in the general case.

We will see below that for a regular linac with constant quadrupole spacing L the formula (8) may be simplified for some correction techniques, in particular for those we have considered in this paper. In fact, phase correlation will appear in such a way that only $\langle x(t,k)\, x^*(t,k-k_{\max})\rangle$ in (8) should be taken into account, thus all functions become one-dimensional. Thus, in this simplified case, the mean squared dispersion is

$$\langle \eta_x^2(t)\rangle = 2 \int_{k_{\min}}^{k_{\max}-k_{\min}} \Big(P(t,k)G(k)\ + \mathcal{P}(t,k)\mathcal{G}(k) \Big) \frac{dk}{2\pi} \tag{16}$$

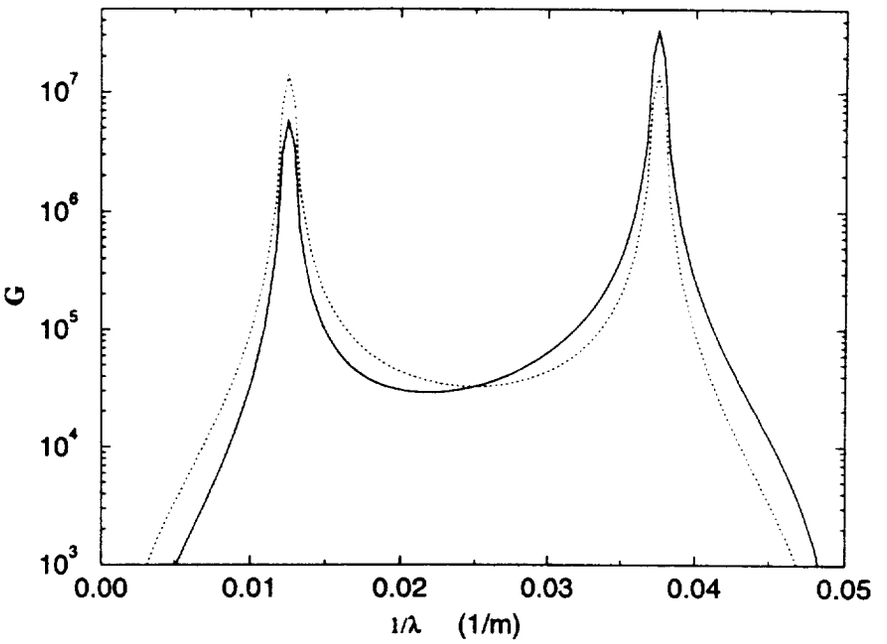

Figure 2: Spectral response functions $G(k)$ (solid line) and absolute value of $\mathcal{G}(k)$ (dashed line, this function is negative). FODO linac, $L = 10$ m, N=128, $\mu = \pi/2$.

where we used the notations

$$\mathcal{P}(t,k) = \lim_{\mathcal{L}\to\infty} \frac{1}{\mathcal{L}} x(t,k)x^*(t,-\tilde{k}) = \lim_{\mathcal{L}\to\infty} \frac{1}{\mathcal{L}} x(t,k)x(t,\tilde{k}) \tag{17}$$

and

$$\mathcal{G}(k) = g_c(k)g_c(\tilde{k}) - g_s(k)g_s(\tilde{k}) \tag{18}$$

In our case $\mathcal{P}(t,k)$ is a real function.

Here and below $\tilde{k} = k_{\max} - k$ and the value $k_{\max} = \pi/L$ corresponds to the shortest wavelength $\lambda = 2L$, which can be produced by misalignments of an infinite regular lattice with spacing L. We take into account in Eq.(16) that the range of integration on k is limited in practice. For the finite regular lattice with spacing L

$$k_{\min} < |k| < k_{\max} - k_{\min} \tag{19}$$

where $k_{\min} = 2\pi/(N\,L)$. Taking integral (16) only for positive k we doubled the result.

One should note that the ground motion spectrum may have any k and the limits in Eq.(10) are infinite, while the spectrum of quadrupole displacements is defined only in certain finite range. This peculiarity is not a contradiction, because, as we will see, all harmonics of ground motion effectively act as if their wavelength values belong to the finite allowed band.

Spectral functions can be easily calculated numerically and even analytically in some cases (see Appendix 1 for more details). A typical plot of $G(k)$ and $\mathcal{G}(k)$

is shown on Fig.2. In this example we choose a regular linac without acceleration, the quadrupole spacing $L = 10$ m, the number of quadrupoles N=128, the phase advance per FODO cell is $\mu = \pi/2$, beta function have maxima in odd quadrupoles.

In short, the spectral response functions $G(k)$ and $\mathcal{G}(k)$ describe the properties of the focusing channel, while the power $P(t,k)$ and the self correlation $\mathcal{P}(t,k)$ spectra will depend on the applied method of correction, initial misalignment and ground motion.

3 Spectral properties of correction techniques

Our aim now is to describe an alignment procedure in terms of evolution of spatial harmonics and then to apply the spectral formalism to different correction techniques.

We consider first the well known "one-to-one " steering algorithm, where BPM readings are used to steer the beam through BPM centers. A variant of this scheme, where the quadrupoles are moved towards the beam line instead of using dipole correctors, is also studied. The "shunt" technique, which can alternatively be used to suppress the BPM offsets is also discussed. Finally the "adaptive alignment" method proposed by V. Balakin [4] will be considered. This method uses BPM readings to repetitively realign quadrupoles to some smooth line.

Some notations have to be introduced before going through the correction methods in more detail. We define $x_{(0)}(k)$ as the k-th harmonics of the vector of initial quadrupole displacements in k-domain, it can be complex. In space domain its components are real values

$$x_{(0)i} \propto \cos(ks_i + \phi) \tag{20}$$

This vector describes the initial misalignment of the elements at $t = 0$. The correction is performed on at $t = \Delta t$ and the resulting quadrupole displacements just after correction are described by harmonics $x_{(1)}(k)$, the value just before correction is $x_{(1-)}(k)$. If correction procedures will be repeated iteratively, one will have $x_{(n)}(k)$ where the index n is the iteration index, which is connected to the time through $t_n = n\Delta t$.

The vector of the BPM offset errors, relative to the quadrupole centers, can be described by the harmonics $z(k)$. These quantities are identical for any iteration n, but are different for different realizations. Last, the vector of BPM resolution errors, due to measurement noise, consists of the harmonics $\xi_{(n)}(k)$, it is different for different n but its spectral properties remains the same.

The effect of ground motion will be given by the harmonics $\psi_{(n)}(k)$ of the vector of quadrupole displacements between the times $t_{n-1} = (n-1)\Delta t$ and $t_n = n\Delta t$.

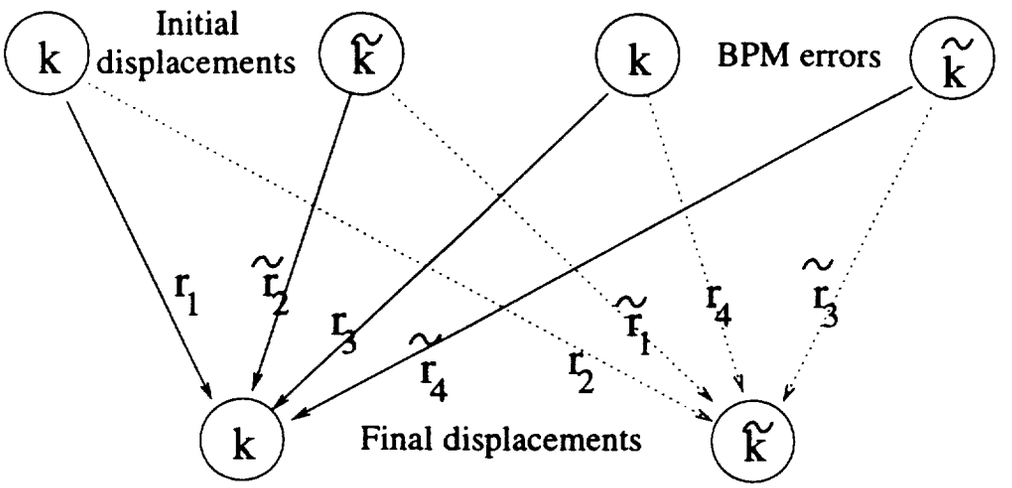

Figure 3: Evolution of spectral harmonics due to alignment procedure.

The correction techniques, which are investigated in this study, introduce phase correlations only between harmonics k and $\tilde{k} = k_{\max} - k$, by the following way. If a term with a phase ϕ arises in the k-th harmonics after correction, some term with a phase $-\phi$ arises also in the $\tilde{k}$-th harmonics. An extension to the more general case can be of course done for other correction methods, which could introduce more complex phase correlations.

We have to express now the change of the harmonics of elements displacement due to a correction procedure (see Fig.3). The coefficients $r_1(k)$ and $r_2(\tilde{k})$ relate the k-th harmonics of the quadrupole position after correction to the k-th and $\tilde{k}$-th harmonics in the initial state. The coefficients $r_3(k)$ and $r_4(\tilde{k})$ give the contribution of the k-th and $\tilde{k}$-th harmonics of the BPM errors to the k-th harmonics of the quadrupole position after correction. In our case these coefficients are real. The k-th harmonics of the quadrupole displacement just after the first correction, at $t = \Delta t$, can then be written as the following

$$\begin{aligned} x_{(1)}(k) &= r_1(k)x_{(0)}(k) + r_2(\tilde{k})x^*_{(0)}(\tilde{k}) + r_3(k)z(k) + r_4(\tilde{k})z^*(\tilde{k}) \\ &+ r_3(k)\xi_{(1)}(k) + r_4(\tilde{k})\xi^*_{(1)}(\tilde{k}) + r_1(k)\psi_{(1)}(k) + r_2(\tilde{k})\psi^*_{(1)}(\tilde{k}) \end{aligned} \quad (21)$$

Assuming that the only correlation originates from the correction procedure, the variance of the quadrupole position after the first correction is

$$\begin{aligned} \langle|x_{(1)}|^2\rangle &= r_1^2\langle|x_{(0)}|^2\rangle + \tilde{r}_2^2\langle|\tilde{x}_{(0)}|^2\rangle + r_3^2\langle|z|^2\rangle + \tilde{r}_4^2\langle|\tilde{z}|^2\rangle \\ &+ r_3^2\langle|\xi|^2\rangle + \tilde{r}_4^2\langle|\tilde{\xi}|^2\rangle + r_1^2\langle\psi_{(1)}\psi^*_{(1)}\rangle + \tilde{r}_2^2\langle\tilde{\psi}_{(1)}\tilde{\psi}^*_{(1)}\rangle \end{aligned} \quad (22)$$

We used abbreviations such as $r_2 = r_2(k)$ and $\tilde{r}_2 = r_2(\tilde{k})$ henceforth. For the self correlation spectrum one gets:

$$\langle x_{(1)}\tilde{x}_{(1)}\rangle = r_1r_2\langle|x_{(0)}|^2\rangle + \tilde{r}_1\tilde{r}_2\langle|\tilde{x}_{(0)}|^2\rangle + r_3r_4\langle|z|^2\rangle + \tilde{r}_3\tilde{r}_4\langle|\tilde{z}|^2\rangle$$

$$+r_3r_4\langle|\xi|^2\rangle \ + \tilde{r}_3\tilde{r}_4\langle|\tilde{\xi}|^2\rangle \ + r_1r_2\langle\psi_{(1)}\psi^*_{(1)}\rangle \ + \tilde{r}_1\tilde{r}_2\langle\tilde{\psi}_{(1)}\tilde{\psi}^*_{(1)}\rangle \qquad (23)$$

Similar equations can be written after many correction processes ($n > 1$). We have to take into account, however, that BPM offset errors of different n are totally correlated, BPM resolution errors are uncorrelated, and ground motion terms $\psi_{(n)}(k)$ of different n may have some correlation.

We assume Gaussian distributions for the initial misalignments and BPM errors and will use spectra instead of variances. The spectra of initial misalignments, static BPM errors (offsets) and stochastic BPM resolution errors are, respectively

$$P_{\rm ini}(k) = L\sigma^2_{\rm ini} = L\langle|x_{(0)}|^2\rangle \qquad (24)$$

$$P_{\rm off}(k) = L\sigma^2_{\rm off} = L\langle|z|^2\rangle \qquad (25)$$

$$P_{\rm res}(k) = L\sigma^2_{\rm res} = L\langle|\xi|^2\rangle \qquad (26)$$

The term corresponding to ground motion $Q_{(i,j)}(k) = L\langle\psi_{(i)}(k)\psi^*_{(j)}(k)\rangle$ can be expressed with the help of Eq.(14). We use the identity

$$(x_1 - x_2)(x_3 - x_4) = \frac{1}{2}\left[(x_1 - x_4)^2 + (x_2 - x_3)^2 - (x_1 - x_3)^2 - (x_2 - x_4)^2\right] \qquad (27)$$

to expand $\psi_{(i)}\psi^*_{(j)}$, remembering that the value $\psi_{(n)}(k)$ in k-domain and the value $x_{\rm abs}(t_n, s) - x_{\rm abs}(t_{n-1}, s)$ in space domain are equivalent. The ground motion term is then

$$Q_{(i,j)}(k) \ = \ \int_{-\infty}^{\infty} P(\omega,k)\left[\cos(\omega(t_i - t_j)) + \cos(\omega(t_{i-1} - t_{j-1}))\right.$$

$$\left. - \cos(\omega(t_i - t_{j-1})) - \cos(\omega(t_{i-1} - t_j))\right]\frac{d\omega}{2\pi}. \qquad (28)$$

This expression assumes that k can run from $-\infty$ to $+\infty$, while the regular lattice with spacing L cannot produce harmonics with very short or very long wavelength. The spectrum of quadrupole displacements has therefore a bounded range. The harmonics of ground motion have hence to be redistributed within the allowed band. For instance, the harmonics with large wave number $mk_{\rm max} + \Delta k$, where m is a positive integer, will effectively appear as $k_{\rm max} - \Delta k$. On the other hand, it is known that long wavelengths do not affect the beam quality and the harmonics with $|k| < k_{\rm min}$ can be simply neglected. The ground motion term is then

$$Q_{(i,j)}(k) \ = \ \int_{-\infty}^{\infty}\left(P(\omega,k) \ + 2L\int_{k_{\rm max}}^{\infty} P(\omega,k)\frac{dk}{2\pi}\right)$$

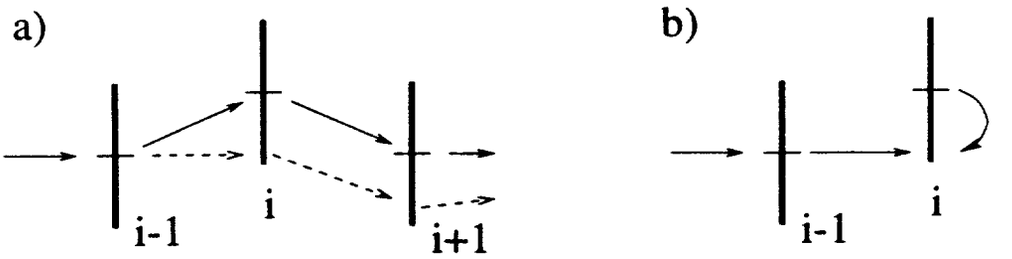

Figure 4: The one to one alignment technique with steering by the previous quadrupole a), and with changing of position of misaligned quadrupole b).

$$\times 2(1-\cos(\omega\Delta t))\cos(\omega(t_i-t_j))\frac{d\omega}{2\pi}, \tag{29}$$

where we assumed that the time interval $\Delta t = t_i - t_{i-1}$ is constant. For the special case of the "ATL law", the expression (29) can be given in a closed form

$$Q_{(i,j)}(k) = \frac{A\Delta t}{2}(1/k_{\max}^2 + 1/k^2)\left(|i-j+1| + |i-j-1| - 2|i-j|\right). \tag{30}$$

In the next chapters, a few correction techniques are studied in more details. The expressions for the resulting power spectra of quadrupole displacements after correction, as well as the final dispersive errors are calculated. Finally, the method is illustrated by some actual examples, which are all based on a same fictitious linac: the number of quadrupoles N=1024, quadrupole spacing $L = 10$ m, phase advance $\mu = 90°$, no acceleration, beta function has maximum in odd quadrupoles, beta function at the exit $\beta_N = 5.86$ m.

4 "One-to-one" correction techniques

The "one-to-one" algorithm consists in zeroing the BPM measurements. This can be done by steering the beam by means of dipole correctors (Fig.4a) or by moving the misaligned quadrupoles towards the beam (Fig.4b). These two methods give different results, they are studied separately.

4.1 "One-to-one" by steering

It is more convenient to our formalism to replace deflections given by dipole correctors by displacements of the associated quadrupoles.

If we suppose the i-th quadrupole is misaligned, three additional angles are needed to re-align the beam. The equivalent quadrupole displacements, which should be subtracted from their initial positions, are then

$$\Delta x_i = -\frac{2x_i}{LK_i} \text{ and } \Delta x_{i+1} = \Delta x_{i-1} = -\frac{x_i}{LK_i} \tag{31}$$

Here K_i is the r_{21} coefficient of the quadrupole transport matrix. The algorithm can therefore be expressed in this way

$$x_i \to x_i + \frac{1}{LK_i}(2x_i - x_{i+1} - x_{i-1}) \tag{32}$$

We assume a regular FODO lattice, where the signs of the quadrupole strengths alternate, $K_i = -K_{i+1}$. We can write it alternatively

$$K_i = K\,\cos(s_i\pi/L) = K\,\cos(k_{\max}s_i) \tag{33}$$

where $s_i = iL$ are the locations of the quadrupoles. Taking $x_i = \cos(ks_i + \phi)$ and using the identity

$$\cos(ks_i + \phi)\cos(k_{\max}s_i) = \cos(k_{\max}s_i - ks_i - \phi) \tag{34}$$

we note that a k-th harmonics of the initial misalignment will produce two harmonics of quadrupole displacements after the correction: k-th and $(k_{\max} - k)$-th with opposite phase. The coefficients $r_1(k)$ and $r_2(k)$, showing the change of the harmonics k and connection with the harmonics $k_{\max} - k$ of the quadrupole displacements after correction, are

$$r_1(k) = 1 \quad \text{and} \quad r_2(k) = \frac{2}{LK}(1 - \cos(kL)) \tag{35}$$

The coefficients $r_3(k)$ and $r_4(k)$, showing the effect of BPM errors, are

$$r_3(k) = 1 \quad \text{and} \quad r_4(k) = \frac{2}{LK}(1 - \cos(kL)) \tag{36}$$

The power spectrum of quadrupole displacements after correction, with ground motion, described by the "ATL law", is thus

$$P(k) = L(\sigma_{\text{ini}}^2 + \sigma_{\text{err}}^2)\left(1 + \left(\frac{2}{LK}\right)^2(1 + \cos(kL))^2\right)$$

$$+ A\Delta t\left(\left(\frac{1}{k^2} + \frac{1}{k_{\max}^2}\right) + \left(\frac{2}{LK}\right)^2(1 + \cos(kL))^2\left(\frac{1}{\tilde{k}^2} + \frac{1}{k_{\max}^2}\right)\right) \tag{37}$$

In the same way, the self correlation spectrum is

$$\mathcal{P}(k) = L(\sigma_{\text{ini}}^2 + \sigma_{\text{err}}^2)\frac{4}{LK}$$

$$+\frac{2A\Delta t}{LK}\left((1 - \cos(kL))\left(\frac{1}{k^2} + \frac{1}{k_{\max}^2}\right) + (1 + \cos(kL))\left(\frac{1}{\tilde{k}^2} + \frac{1}{k_{\max}^2}\right)\right) \tag{38}$$

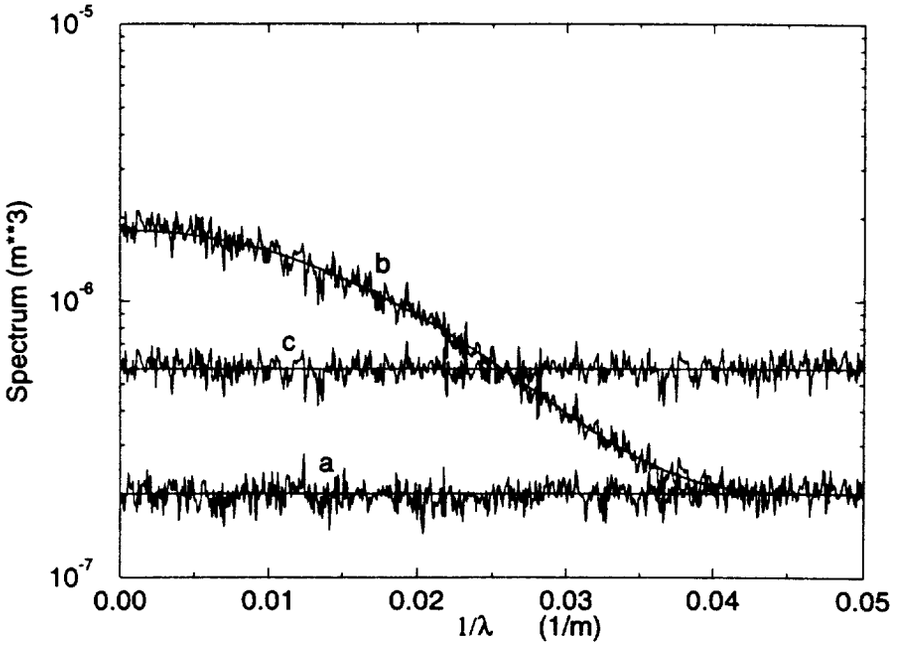

Figure 5: Initial power spectrum (a), and spectra after one to one correction by steering, power spectrum (b) and self correlation (c). Simulations in comparing with analytical results (smooth curves). Initial misalignment $\sigma_{\rm ini} = 100\mu$m. No BPM errors. The spectra here, as well as on the others pictures showing spectra, are doubled in comparing with formulas in the text.

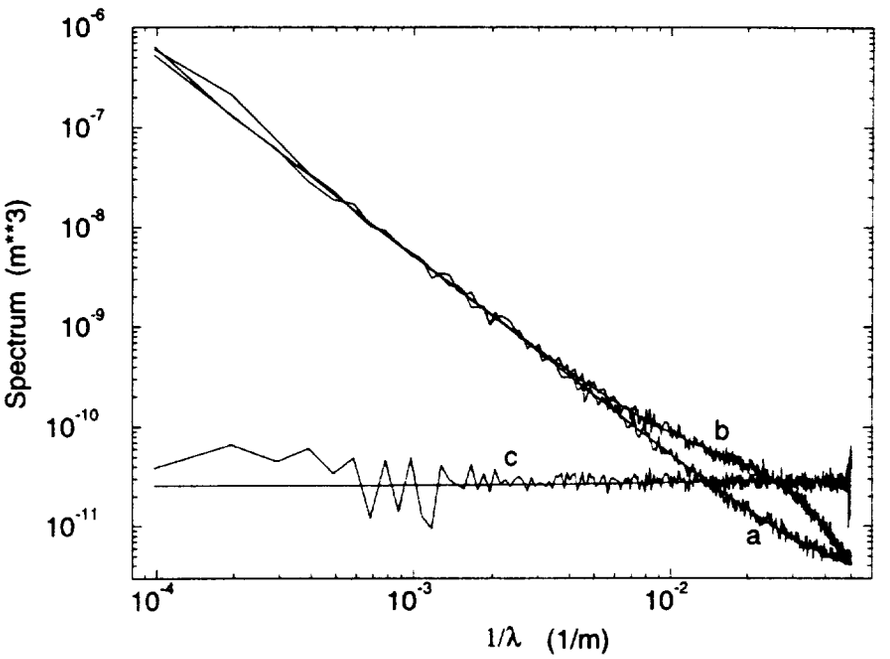

Figure 6: Power spectrum just before (a) and after one to one correction by steering (b – power, c – self correlation). Ground motion by "ATL law" with $A\Delta tL = 10^{-12}$ m^2. No initial misalignment, no BPM errors.

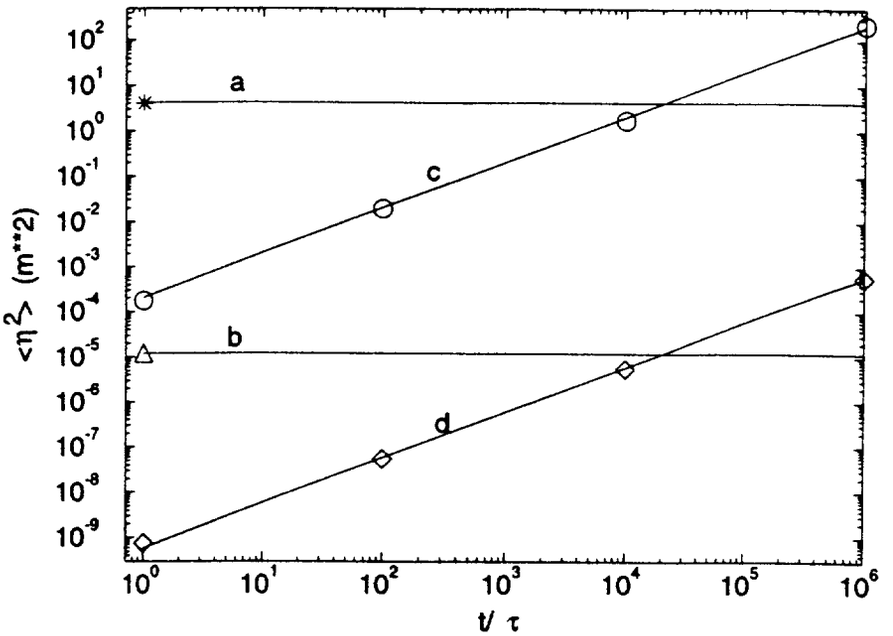

Figure 7: The mean squared dispersion for the "one-to-one" correction by dipole steering, a) and b) - with initial misalignment $\sigma_{\rm ini} = 100$ μm solely (before and after correction), c) and d) - with "ATL" ground motion solely (before and after correction), $\tau = 10^{-12}$ m$^2/(AL)$.

The quantity $\sigma_{\rm err}$ means here the total rms BPM error, including both BPM offset and BPM resolution ($\sigma^2_{\rm err} = \sigma^2_{\rm off} + \sigma^2_{\rm res}$).

One can note that, without ground motion, the power spectrum after correction does not grow for small k, meaning that the smooth deviation of the line of quadrupoles, a typical feature of the other correction methods, is not significant for this correction technique. On the other hand, the power spectrum of the quadrupole displacements is larger after correction than before correction.

Taking ground motion into account, we reasonably assumed that the time, required for the change of the corrector settings, is smaller than the characteristic time of the emittance growth due to ground motion. When the correction procedure is iteratively repeated, the spectra are still given by the expressions (37) and (38), but the ground motion terms have to be multiplied by n. A few examples of spectra obtained with analytical formulas and compared to numerical simulations are shown on Fig.5 and Fig.6.

The dispersion can be found by use of (37,38), provided that injection conditions are correctly specified (see Appendix 2). Alternatively, one can show that for the "one-to-one" corrections the dispersive error can be written

$$\langle \eta_x^2(t) \rangle = 2 \int_{k_{\rm min}}^{k_{\rm max}} \hat{P}(t,k)\, \hat{G}(k)\, \frac{dk}{2\pi} \qquad (39)$$

where $\hat{G}(k)$ and $\hat{P}(t,k)$ are the effective spectral response function and the ef-

fective spectrum of quadrupole displacements before correction respectively. The $\hat{G}(k)$ is built according to (11,12) with new dispersive coefficients

$$\hat{d}_i = d_i + (2d_i + d_{i+1} + d_{i-1})/(LK_i) \tag{40}$$

and $\hat{P}(t,k)$ is given by

$$\hat{P}(t,k) = L(\sigma_{\rm ini}^2 + \sigma_{\rm err}^2) + A\Delta t\left(1/k^2 + 1/k_{\rm max}^2\right) \tag{41}$$

It is useful to note that if there is no acceleration, then

$$\hat{d}_i = -K_i r_{12}^i \tag{42}$$

The rms dispersive error versus time can then be calculated with the formulae (107) or (39), they give the same result. For example, Fig.7 shows the results obtained with analytical formula (straight lines) and with numerical simulations with particle tracking (symbols): on the fictitious linac, previously described: with initial misalignment solely (curves a and b, before and after correction), and with ground motion solely (curves c and d, before and after correction). These last curves can help to choose the needed repetition rate of the re-alignment of the linac, once the maximum allowed emittance growth is fixed. The analytical results exhibits the following approximate dependencies before and after correction, respectively:

$$\langle \eta_x^2 \rangle \approx (\sigma_{\rm ini}^2 + 0.5A\Delta tL)\,0.3N^3 \tag{43}$$

$$\langle \eta_x^2 \rangle \approx (\sigma_{\rm ini}^2 + \sigma_{\rm err}^2 + 0.5A\Delta tL)\,1.2N \tag{44}$$

These equations are in fact particular cases of the following general expressions, which can be obtained using Eq.(39) and formulae shown in Appendix 1. The dispersion error in the linac without corrections:

$$\langle \eta_x^2 \rangle \approx (\sigma_{\rm ini}^2 + \sigma_{\rm err}^2 + AtL/2)\,(\beta_{\rm max} + \beta_{\rm min})\beta_N K^2 \tan^2(\mu/2)N^3/16 \tag{45}$$

The dispersion error in the linac with corrections, at the moment just after correction:

$$\langle \eta_x^2 \rangle \approx (\sigma_{\rm ini}^2 + \sigma_{\rm err}^2 + AtL/2)\,(\beta_{\rm max} + \beta_{\rm min})\beta_N K^2 N/4 \tag{46}$$

They are valid without acceleration, however similar formulae can also be found with the help of Appendix 1 taking acceleration in the linac into account.

We see from these expressions that "ATL" ground motion causes linear growth of the dispersion error with time. If corrections are applied, the dispersion error is reduced by the factor of N^2 approximately, but still grows linearly with time. Thus, after some time, some beam based alignment technique should be used to realign the quadrupoles.

4.2 "One-to-one" by quadrupole moving

The beam will now be passed through the center of the i-th BPM by moving the i-th quadrupole. The resulted quadrupole misalignments will not depend on the initial quadrupole positions, but only on the total BPM errors. If a_j is here the total BPM error of the j-th element, then the position of the i-th element after alignment will be

$$x_i = -a_i + \sum_{j=1}^{i-1} K_j a_j (s_i - s_j) \tag{47}$$

Considering one harmonics of the BPM errors $a_i = \cos(ks_i + \phi)$ and performing summation in (47), one gets

$$x_i = -\cos(ks_i + \phi) - \frac{KL}{2(1 + \cos(kL))}$$

$$\times \left(\cos(\pi i)\cos(ks_i + \phi) + i\cos(kL + \phi) + (i-1)\cos(\phi)\right) \tag{48}$$

From the spectral point of view the constant or linear on i terms can be neglected. The coefficients accounting for the quadrupole displacements caused by initial misalignments are zero:

$$r_1(k) = 0 \ , \quad r_2(k) = 0 \tag{49}$$

The coefficients accounting for the BPM errors are

$$r_3(k) = -1 \ , \ r_4(k) = -\frac{KL}{2(1 + \cos(kL))} \tag{50}$$

The power spectrum of quadrupole displacement after correction can be easily deduced

$$P(k) = L\sigma_{\text{err}}^2 \left(1 + \frac{(KL)^2}{4(1 - \cos(kL))^2}\right) \tag{51}$$

In the same way, the self correlation spectrum is

$$\mathcal{P}(k) = L\sigma_{\text{err}}^2 \frac{KL}{\sin^2(kL)} \tag{52}$$

where σ_{err} is again the total BPM error, which includes offset and resolution errors ($\sigma_{\text{err}}^2 = \sigma_{\text{res}}^2 + \sigma_{\text{off}}^2$).

Since the spectra after correction do not depend on initial position of quadrupoles, and with the assumption that the time, required for moving the quadrupoles is smaller than the characteristic time of emittance growth due to ground motion, the correction and the ground motion are here completely dissociated.

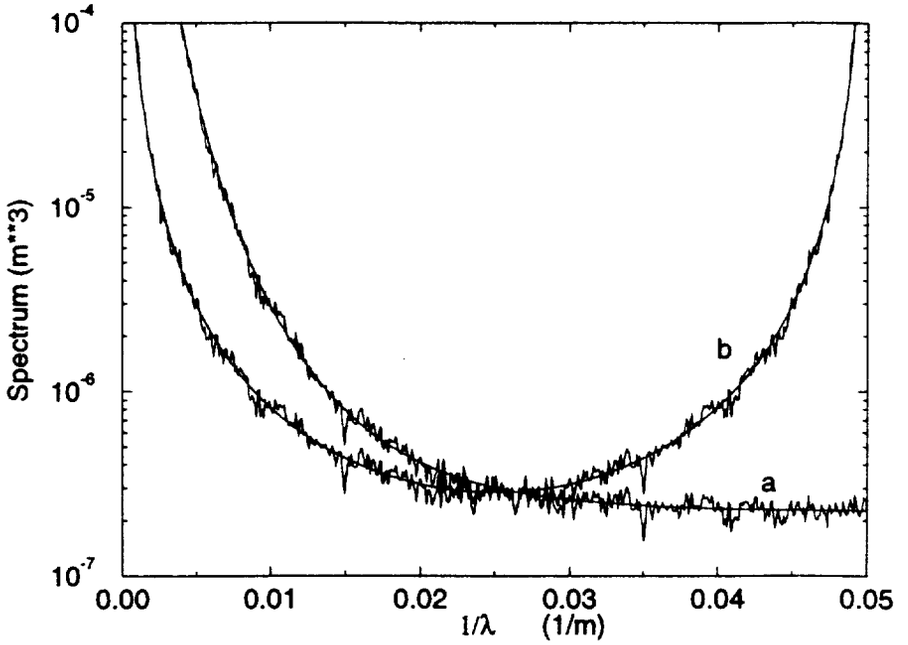

Figure 8: Power (a) and self correlation (b) spectra after one to one correction by quadrupole moving. $\sigma_{\rm err} = 100$ μm.

In order to find dispersion correctly, one need to take into account all terms in (48), see Appendix 2. In the same way as before, one can alternatively introduce new coefficients

$$\hat{d}_i = -d_i + K_i \sum_{j=i+1}^{N} d_j(s_j - s_i) \tag{53}$$

to build the effective $\hat{G}(k)$. The effective spectrum in this case is

$$\hat{P}(k) = L\sigma_{\rm err}^2 \tag{54}$$

We note that without acceleration the dispersive coefficient is again

$$\hat{d}_i = -K_i r_{12}^i \tag{55}$$

as for the previous method. However, with acceleration the coefficients $\hat{d}_i$ for these two methods are different.

The rms dispersive error can again be calculated with the help of the formulae (107) or (39). Unlike the corrector steering method, we note that the power spectrum after correction grows for small k as $1/k^4$, leading to a smooth deviation of the quadrupoles line from their original position. It is also seen, of course, directly from (48). In spite of this spectrum divergence the answer is finite because the bounds of integration are cut at $k_{\rm min}$ and $k_{\rm max} - k_{\rm min}$. Moreover, contribution of this tails mostly cancels in (107) during integration.

The analytical results, confirmed by particle tracking, exhibit the following approximate dependencies of the dispersive error after correction for our fictitious linac:

$$\langle \eta_x^2 \rangle \approx \sigma_{\rm err}^2 \, 1.2N \tag{56}$$

which shows the same dependence on the BPM errors as the previous method. The previous formula is the particular case of the next general expression, which is valid if there is no acceleration

$$\langle \eta_x^2 \rangle \approx \sigma_{\rm err}^2 (\beta_{\rm max} + \beta_{\rm min}) \beta_N K^2 N/4 \tag{57}$$

This formula was obtained by using Eq.(39) and formulae of Appendix 1.

One can note that the so-called "shunt" method (used, for example, to align the FFTB beam line [6]), which suppress effectively the BPM offsets, can be described by the same equations. This method is rather a beam-based alignment technique and cannot be used directly as a continuous-time feedback, because different quadrupole settings are needed. It requires to move a quadrupole in such a way that changing of its strength does not produce beam shift in the next BPM. This procedure repeats step by step for all quadrupoles and the final dispersive error is only limited by the BPM resolution. If the relative strength changing is $\delta_K = \delta K/K$ then the precision of cancelation of the BPM offset is $\sigma_{\rm res}/(KL\,\delta_K)$. The spectra of the quadrupoles after alignment will be defined by Eqs.(51, 52, 114 or 54) where the total BPM errors mean now $\sigma_{\rm err}^2 = \sigma_{\rm res}^2(1 + 1/(KL\,\delta_K)^2)$.

5 The "adaptive alignment" method

The algorithm, proposed in [4], calculates from the readings a_i of three neighboring BPMs the change of position of the central quadrupole

$$\Delta x_i = c_0 \frac{1}{3} [a_{i+1} + a_{i-1} - a_i(2 + K_i L)] \tag{58}$$

The coefficient c_0 controls the velocity of convergence of the algorithm. This procedure is normally repeated iteratively.

Let us suppose that only one quadrupole is misaligned with the unity displacement $x_i = 1$ and that the BPMs are perfect, i.e. they have no offsets or measurement errors. One can show that at the first iteration only three quadrupoles have non zero correction:

$$\Delta x_{i-1} = \Delta x_{i+1} = -\frac{1}{3} c_0, \qquad \Delta x_i = \frac{2}{3} c_0 \tag{59}$$

The position of the i-th quadrupole after the first iteration is then

$$x_{(1)i} = x_{(0)i} - \frac{1}{3} c_0 \left(2x_{(0)i} - x_{(0)i+1} - x_{(0)i-1}\right) \tag{60}$$

The coefficients, accounting for the quadrupole displacements caused by this correction, can then be deduced

$$r_1(k) = 1 - \frac{2}{3} c_0 (1 - \cos(kL)) \quad \text{and} \quad r_2(k) = 0 \tag{61}$$

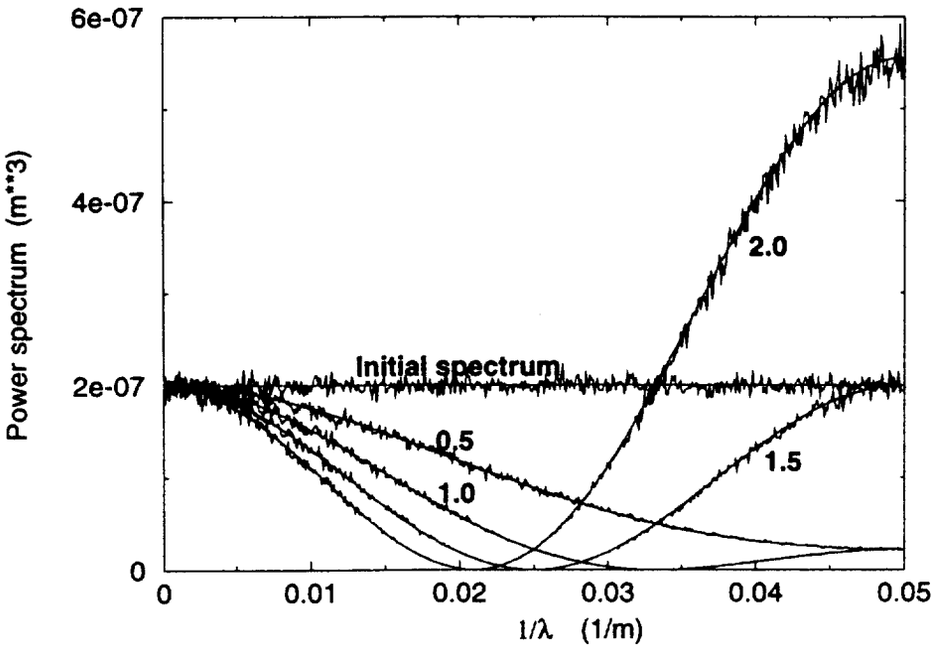

Figure 9: Power spectrum after first iteration of the "adaptive alignment" method, no BPM errors, numbers shows the value of coefficient c_o. Initial misalignment $\sigma_{\rm ini} = 100\mu$m.

Even after the first iteration, some harmonics, for which $r_1 = 0$, will be damped completely. If the coefficient c_0 is too large ($> 3/2$), the damping condition ($r_1 < 1$) is no longer valid and the algorithm will finally diverge.

Let us assume now that all quadrupoles are perfectly aligned but BPMs have errors. A harmonics of BPM signals, $a_i = \cos(ks_i + \phi)$, gives the correction to be applied at the first iteration:

$$\Delta x_i = -\frac{2}{3}c_0(1 - \cos(kL))\,\cos(ks_i + \phi) - \frac{1}{3}c_0\,K_i\,L\,\cos(ks_i + \phi) \qquad (62)$$

We note again that the k-th harmonics of BPM errors will generate two harmonics (k and $(k_{\rm max} - k)$) of quadrupole displacements after the first iteration. The coefficients accounting for the BPM errors are then:

$$r_3(k) = -\frac{2}{3}c_0(1 - \cos(kL)) \text{ and } r_4(k) = -\frac{1}{3}c_0 KL \qquad (63)$$

If we consider now an arbitrary number of iterations, successive equations have to be written. We obtain for the k-th harmonics after the n-th iteration (taking into account the equality $r_2 = 0$):

$$x_{(n)}(k) \;=\; r_1^n x_0 + \sum_{i=1}^{n} r_1^{n-i} r_3 z + \sum_{i=1}^{n} r_1^{n-i} \tilde{r}_4 \tilde{z}^*$$

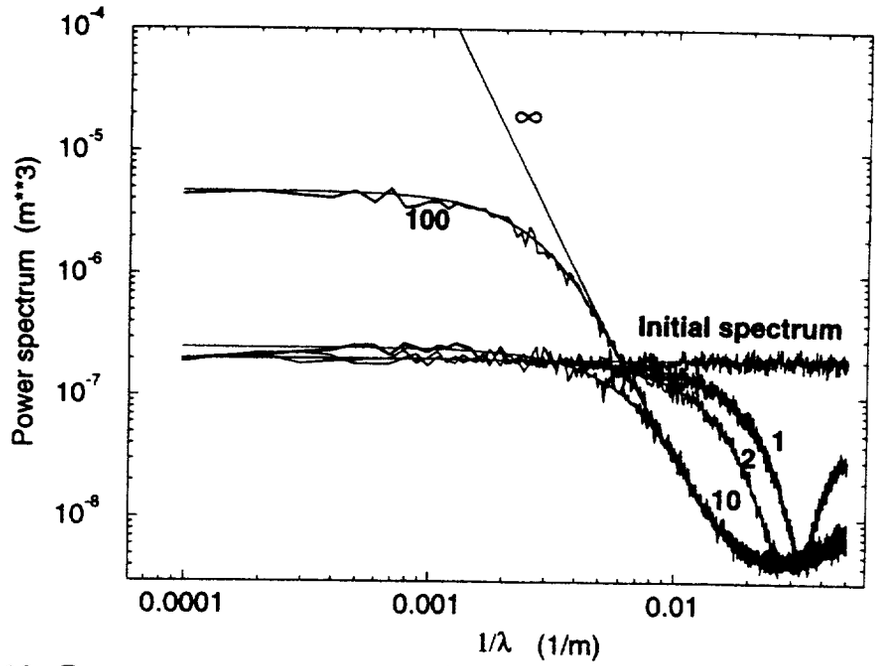

Figure 10: Power spectrum versus number of iterations for the "adaptive alignment" method, with random and static BPM errors, numbers shows the number of iterations. Initial misalignment $\sigma_{\rm ini} = 100\mu$m, BPM errors $\sigma_{\rm res} = \sigma_{\rm off} = 10\mu$m.

$$+\sum_{i=1}^{n} r_1^{n-i} r_3 \xi_{(i)} + \sum_{i=1}^{n} r_1^{n-i} \tilde{r}_4 \tilde{\xi}^*_{(i)} + \sum_{i=1}^{n} r_1^{n-i} r_1 \psi_{(i)} \tag{64}$$

The variance of the k-th harmonics of the total quadrupole displacement after the n-th iteration is then

$$\langle |x_{(n)}|^2 \rangle = r_1^{2n} \langle |x_0|^2 \rangle + \langle |z|^2 \rangle \sum_{i=1}^{n}\sum_{j=1}^{n} r_1^{2n-i-j} r_3^2 + \langle |\tilde{z}|^2 \rangle \sum_{i=1}^{n}\sum_{j=1}^{n} r_1^{2n-i-j} \tilde{r}_4^2$$

$$+\langle |\xi|^2 \rangle \sum_{i=1}^{n} r_1^{2n-2i} r_3^2 + \langle |\tilde{\xi}|^2 \rangle \sum_{i=1}^{n} r_1^{2n-2i} \tilde{r}_4^2 + \sum_{i=1}^{n}\sum_{j=1}^{n} r_1^{2n-i-j} r_1^2 \langle \psi_{(i)} \psi^*_{(j)} \rangle \tag{65}$$

The sums in (65) represent geometric progressions and can be calculated easily. The spectrum of self correlation can be found in a similar way.

After simplifications, the power spectrum of quadrupole displacements is the following

$$P_{(n)} = r_1^{2n} P_{\rm ini} + (r_3^2 + \tilde{r}_4^2) \left(P_{\rm off} \frac{(1-r_1^n)^2}{(1-r_1)^2} + P_{\rm res} \frac{(1-r_1^{2n})}{(1-r_1^2)} \right)$$

$$+\sum_{i=1}^{n}\sum_{j=1}^{n} r_1^{2n-i-j} r_1^2 Q_{(i,j)} \tag{66}$$

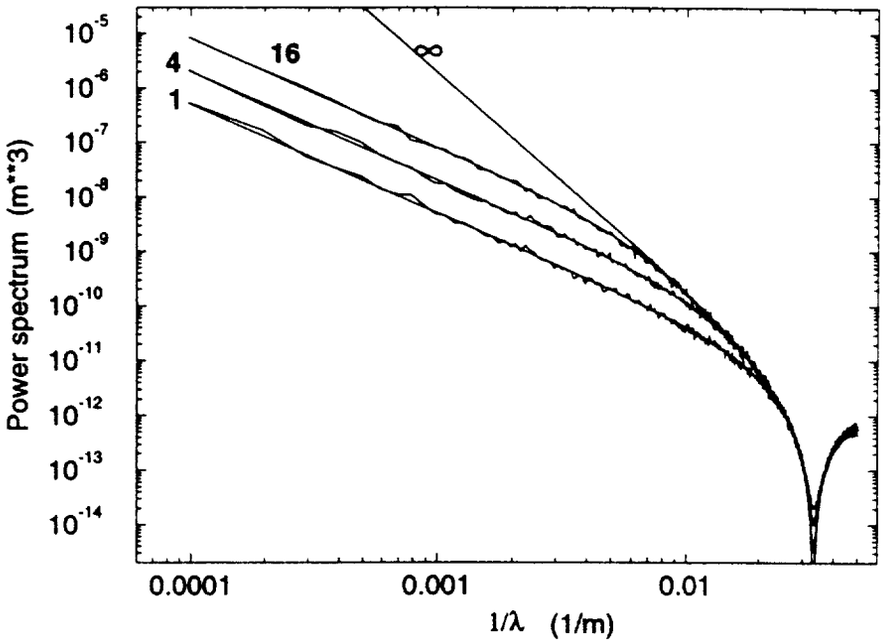

Figure 11: Power spectrum versus number of iterations for the "adaptive alignment" method, numbers shows the number of iterations, Ground motion by "ATL law" with $A\Delta t L = 10^{-12}$ m^2. No initial misalignment, no BPM errors.

In the same way, the self correlation is

$$\mathcal{P}_{(n)}(k) = (r_3\tilde{r}_4 + r_4\tilde{r}_3)\left(P_{\text{off}}\left(\frac{1-r_1^n}{1-r_1}\right)\left(\frac{1-\tilde{r}_1^n}{1-\tilde{r}_1}\right) + P_{\text{res}}\left(\frac{1-(r_1\tilde{r}_1)^n}{1-r_1\tilde{r}_1}\right)\right) \quad (67)$$

For the special case, where the "ATL law" is used to describe the ground motion, the last term in (66) is

$$r_1^2\sum_{i=1}^{n}\sum_{j=1}^{n} r_1^{2n-i-j}Q_{(i,j)} = A\Delta t\left(\frac{1}{k_{\text{max}}^2} + \frac{1}{k^2}\right) r_1^2\frac{1-r_1^{2n}}{1-r_1^2} \quad (68)$$

If the coefficient r_1 is lower than one for any k, then the algorithm is converging and the power spectrum after an infinite number of iterations can be explicitly expressed. Taking again the "ATL law" for the ground motion, we obtain the following power spectrum

$$P_{(\infty)}(k) = (r_3^2 + \tilde{r}_4^2)\left(\frac{P_{\text{off}}}{(1-r_1)^2} + \frac{P_{\text{res}}}{(1-r_1^2)}\right) + A\Delta t\left(\frac{1}{k_{\text{max}}^2} + \frac{1}{k^2}\right)\frac{r_1^2}{1-r_1^2} \quad (69)$$

The self correlation spectrum is obtained in the same way

$$\mathcal{P}_{(\infty)}(k) = (r_3\tilde{r}_4 + r_4\tilde{r}_3)\left(\frac{P_{\text{off}}}{(1-r_1)(1-\tilde{r}_1)} + \frac{P_{\text{res}}}{(1-r_1\tilde{r}_1)}\right) \quad (70)$$

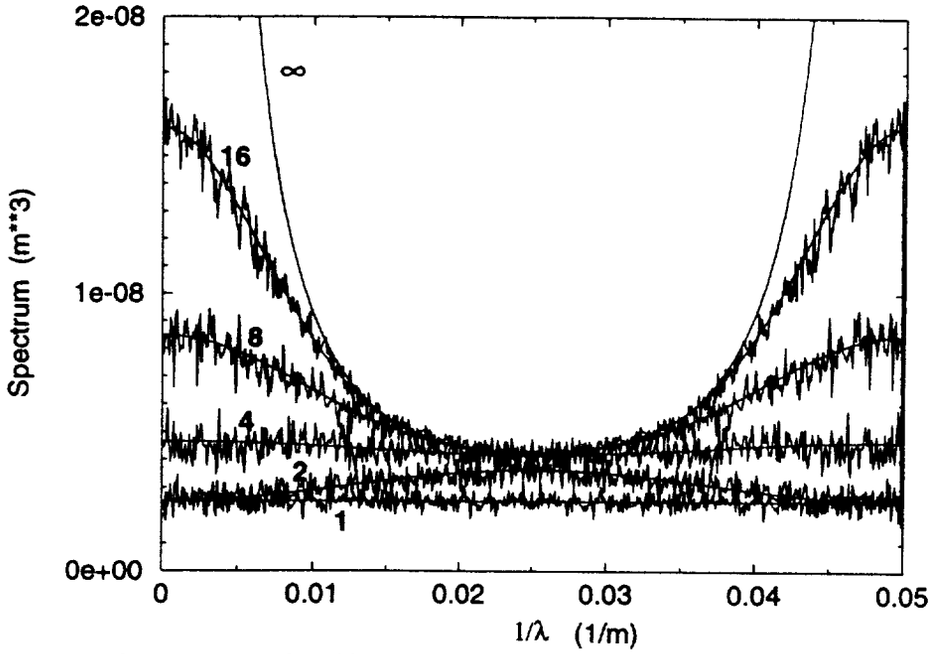

Figure 12: Spectrum of self correlation $\mathcal{P}(k)$ for the "adaptive alignment" method. Numbers shows number of iterations. Static and random error $\sigma_{\text{off}} = 10\mu\text{m}$, $\sigma_{\text{res}} = 10\mu\text{m}$. No initial misalignment, no ground motion.

The figure Fig.9 shows, for example, the power spectra given by simulations and by analytical expressions (smooth curves) just after the first iteration. An initial quadrupole misalignment of $\sigma_{\text{ini}} = 100\mu\text{m}$ and no BPM errors were chosen. One can see a clear divergence for harmonics with small wavelengths when the control coefficient c_0 is too large ($> 3/2$). An optimal value can also be deduced. One can show that the ratio of the integral of initial spectrum to the integral of the spectrum after first iteration has a maximum at $c_0 = 1$. We assume $c_0 = 1$ henceforth.

Power spectra with different number of iterations are shown on the figure Fig.10, where, in addition to a quadrupole misalignment ($\sigma_{\text{ini}} = 100\mu\text{m}$), BPM offset and resolution errors ($\sigma_{\text{off}} = \sigma_{\text{res}} = 10\mu\text{m}$) have been introduced. As predicted by Eq.(66), the left side of the figure, i.e. for the long wavelengths, is dominated by the effects of the offset errors, while the right side, i.e. for short wavelengths, is dominated by the resolution errors of the BPMs. On the Fig.11, the ground motion solely is taken into account, without initial quadrupole misalignment and without BPM errors. For these two figures, we observe that short wavelength harmonics are quickly stabilized, while more time is required for the long wavelength harmonics. For two cases, for offset BPM errors or for ground motion, the power spectrum after a big enough number of iterations scales like $1/k^4$ at small k, like for the "one-to-one" correction by moving the quadrupoles.

The figure Fig.11 shows the self correlation spectrum for different number of

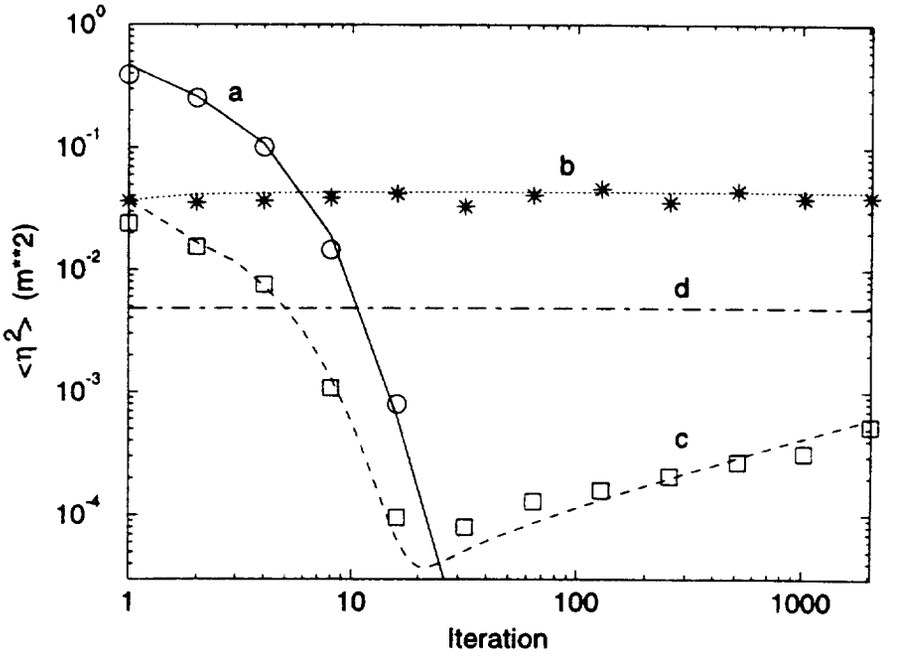

Figure 13: Mean squared dispersion versus number of iterations for the "adaptive alignment" method. a) - initial misalignment $\sigma_{\rm ini} = 100\mu$m solely; b) - BPM random errors $\sigma_{\rm res} = 10\mu$m solely; c) - BPM static errors $\sigma_{\rm off} = 10\mu$m solely; d) - the limit at $n \to \infty$ of the case c).

iterations (without initial misalignment and ground motion, but with BPM errors $\sigma_{\rm off} = \sigma_{\rm res} = 10\mu$m). Numerical simulations and analytical formula (smooth curves) are in excellent agreement.

When displacements are produced by ground motion solely, the equilibrium value (i.e. at $t \to \infty$ or when no dependence on n occurs) of the dispersive error can be expressed in terms of two other functions $F(\omega, k)$ and $H(\omega, k)$, which are the characteristic functions of the correction method:

$$\langle \eta_x^2 \rangle_\infty = \int_{-\infty}^{\infty} \int_{-\infty}^{\infty} \left(G(k) F(\omega, k) + \mathcal{G}(k) H(\omega, k) \right) P(\omega, k) \frac{d\omega}{2\pi} \frac{dk}{2\pi} \qquad (71)$$

One can find the functions $F(\omega, k)$ and $H(\omega, k)$ for this alignment method. Comparing this with Eq.(66), changing limits of sums and neglecting fast oscillating terms will yield in the following expression

$$F(\omega, k) = \sum_{i=0}^{\infty} r_1^{2i} \left(1 - \cos(\omega \Delta t)\right) \qquad (72)$$

where we assume that contribution of $|k| > k_{\rm max}$ can be neglected. It is then

$$F(\omega, k) = \frac{3\left(1 - \cos(\omega \Delta t)\right)}{2c_0 \left(1 - \cos(kL)\right)}. \qquad (73)$$

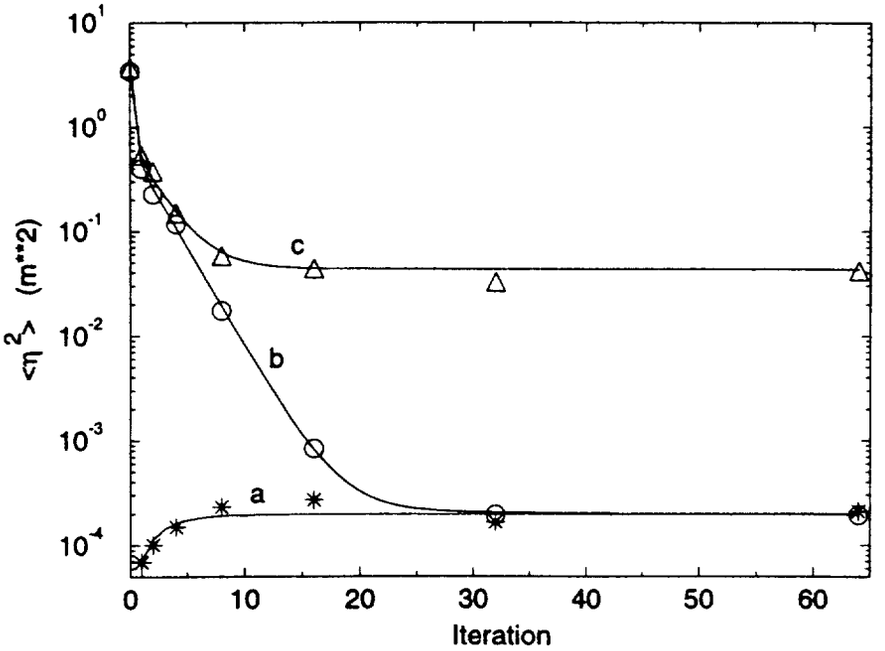

Figure 14: Mean squared dispersion versus number of iterations for the "adaptive alignment" method, no BPM errors. a) ground motion by "ATL law" with $A\Delta tL = 10^{-12}$ m^2 solely; b) ground motion and initial misalignment with $\sigma_{\rm ini} = 100\mu$m; c) ground motion, initial misalignment and BPM errors $\sigma_{\rm res} = \sigma_{\rm off} = 10\mu$m.

This function shows again that frequencies $\omega \ll 1/\Delta t$ of the power spectrum $P(\omega, k)$ damped as ω^2, while small k increased as $1/k^2$ due to considered alignment technique. $H(\omega, k) = 0$ for this method. One can also see that for the "one-to-one" by steering $F(\omega, k) = \infty$ and for the "one-to-one" by moving $F(\omega, k) = 0$.

When all power spectra are available, one can use equation (16) with spectral function based on (12) to find dispersion error. The results of simulations (particle tracking) in comparing with analytical results are shown in Fig.13 and Fig.14.

One can see that the effect of initial misalignments is damped after some tens of iteration, the effect of ground motion stabilizes after a few iterations, the effect of BPM resolution errors is almost constant and the effect of BPM offset errors requires thousands iterations.

The equilibrium value of dispersion error exhibits the following numerical dependence

$$\langle \eta_x^2 \rangle_\infty \approx (0.33\sigma_{\rm res}^2 + 0.05\sigma_{\rm off}^2 + 0.2A\Delta tL)\, N^3 \qquad (74)$$

The analytical expression can also be found by using Appendix 1, however it is too long to be shown here.

As we see, the dispersion error after the "adaptive alignment" still scales like N^3, as was before alignment, while the "one-to-one" methods give $\langle \eta_x^2 \rangle \propto N$. The reason is that for "one-to-one" the orbit is really controlled, it is kept close

to the quadrupole (or BPM) centers. One can imagine that in practice the angle and position of the injected beam could be adjusted in the "adaptive alignment" in order to make use of the smoothness of the aligned line thus decreasing the dispersive errors.

In contrast to the "one-to-one" by steering method, ground motion does not cause permanent growth of dispersive error if the "adaptive alignment" is continuously applied. Thus, this method can be used solely, it does not require periodic realignments of the linac by a special procedure. However, this method may require more precise BPMs.

6 Conclusion

We have shown that the chromatic dilution in future linear colliders can be calculated analytically taking all important effects, namely initial misalignment, any sophisticated ground motion, alignment procedures, into account. The used spectral approach is the natural extension of the $P(\omega, k)$ spectrum concept, which was previously introduced to describe ground motion.

A few correction methods, such as well known "one-to-one" techniques, as well as more recent "adaptive alignment" method have been investigated in the framework of presented approach. The analytical results are in perfect agreement with the results obtained by particle tracking. A regular linac, having a constant spacing of the focusing elements, is the only limitation we saw in this spectral method. The presented results will help to study alignment techniques of the future linear collider, to choose a proper technique and determine its necessary parameters [7].

The most important advantage of the spectral approach is the possibility to evaluate the performance of correction techniques dynamically.

Acknowledgement

The authors would like to thank Reinhard Brinkmann, Vladimir Shiltsev and Nick Walker for useful discussions.

References

[1] V. Juravlev, P. Lunev, A. Sery, A. Sleptsov, K. Honkavaara, R. Orava, E. Pietarinen, "Seismic Conditions in Finland and Stability Requirements for the Future Linear Collider", HU-SEFT R 1995-01, Helsinki (1995).

[2] A. Sery, O. Napoly, "Influence of Ground Motion on the Time Evolution of Beam in Linear Colliders", DAPNIA/SEA/95-04, CE Saclay, (1995); Phys. Rew. E. **53**, 5323, (1996).

[3] K. Thompson, T. Himel, S. Moore, L. Sanchez-Chopitea, H. Shoaee, "Operational Experience with Model-Based Steering in the SLC Linac" PAC 89, Chicago (1989).

[4] V. Balakin, "Adaptive Structure VLEPP", Proc. of 3rd Intern. Workshop on Next Generation Linear Collider LC91, Protvino, (1991).

[5] B. A. Baklakov, P. K. Lebedev, V. V. Parkhomchuk, A. A. Sery, A. I. Sleptsov, V. D. Shiltsev, "Exploration of Correlation and Power Characteristics of Earth Surface Motion at the UNK Site", INP Report 91-15, (1991), (in Russian); Proc. of 1991 IEEE Part. Accel. Conf., San-Francisco, 3273 (1991); Tech. Ph. **38**, 894, (1993).

[6] P. Tenenbaum, D. Burke, R. Helm, J. Irwin, P. Raimondi, K. Oide, K. Flottman, "Beam-Based Magnetic Alignment of the Final Focus Test Beam" SLAC Report SLAC-PUB-95-6769, (1995).

[7] A. Sery, A. Mosnier, "New Studies of Emittance Growth and Correction Techniques for the TESLA Linac", submitted to EPAC 96, (1996).

Appendix 1

In this section some properties of the spectral response functions are considered. Presented formulae allow to find approximate values of coefficients b_i and d_i, positions of resonances and values in the resonances of the spectral functions.

In thin lens approximation the quadrupole displaced by x_i produces an angular kick $\theta = -K_i x_i$ and the resulting offset at the exit is $x^* = -r^i_{12} K_i x_i$ where K_i is the integrated strength of the quadrupole (in our definition it equals to r_{21} of the quadrupole matrix), r^i_{12} is the coefficient of the transfer matrix from the i-th element to the exit. Therefore the coefficient b_i is equal to

$$b_i = -K_i\, r^i_{12} \tag{75}$$

The coefficient d_i is the derivative of (75) with respect to the energy deviation δ:

$$d_i = \frac{d}{d\delta} b_i = \frac{d}{d\delta} \left(\frac{K_i}{1+\delta} r^i_{12}(\delta) \right) \tag{76}$$

which is equal to

$$d_i = K_i\, (r^i_{12} - t^i_{126}) \tag{77}$$

where t^i_{126} is the coefficient of the second order transfer matrix from the i-th element to the exit.

The coefficients b_i and d_i follow certain rules, which can be found in the next way. By considering a rigid displacement of the whole beam line, it is easy to find the identity

$$\sum_{i=1}^{N} b_i = 1 - R_{11} \quad \text{and} \quad \sum_{i=1}^{N} d_i = -T_{116} \tag{78}$$

From the other hand, one can show by tilting the whole beam line by a constant angle that the coefficients satisfy for thin lenses to the following identity

$$\sum_{i=1}^{N} b_i s_i + R_{12} = s_{\text{exit}} \quad \text{and} \quad \sum_{i=1}^{N} d_i s_i + T_{126} = 0 \tag{79}$$

where s_{exit} is the coordinate of the exit and we assume that the entrance coordinate is zero $s_0 = 0$. These rules allow to find behavior of the spectral functions (12) at small k:

$$g_c(k \to 0) \approx \mathrm{O}(k^2) \tag{80}$$

and

$$g_s(k \to 0) \approx -kT_{126} + \mathrm{O}(k^3) \tag{81}$$

Behavior at the right allowed edge $k \to \pi/L$ can be found by considering the equivalent lattice (FOFO instead of FODO, for example) at $k \to 0$.

Let us consider now the case of the regular FODO linac and assume that the quadrupole strength is

$$K_i = K(-1)^i \tag{82}$$

and position of the quadrupoles is

$$s_i = iL \tag{83}$$

where $i = 1, \ldots, N$, the entrance position is zero, the exit position is NL. We denote μ to be the betatron phase advance of the FODO cell, which satisfy to the following equation

$$2\sin(\mu/2) = |K|\, L \tag{84}$$

The matrix element r^i_{12} from i-th quadrupole to the exit is given by

$$r^i_{12} = \sqrt{\beta_i \beta_N}\sin(\psi_i)\sqrt{\frac{\gamma_i}{\gamma_N}} \tag{85}$$

where $\psi_i = \mu/2(N - i)$ is the phase advance between i-th quadrupole and the exit, β_i and β_N are the beta functions at the i-th quadrupole and at the exit respectively, and γ_i is the relativistic Lorentz factor.

The values of the beta functions for the regular FODO linac are the following

$$\beta_{\mathrm{max,min}} = \frac{L}{\tan(\mu/2)(1 \mp \sin(\mu/2))} \tag{86}$$

If K_i is positive (i.e. the quadrupole is defocusing) then $\beta_i = \beta_{\mathrm{min}}$ and vice versa.

Since the energy dependence comes mainly from the phase advance and the beta function variation can be neglected, the coefficient t^i_{126} is given by

$$t^i_{126} \approx -r^i_{12}(N-i)\frac{\tan(\mu/2)}{\tan(\psi_i)} \tag{87}$$

The spectral functions (12) can then be explicitly written:

$$g_s(k) \approx \sum_{i=1}^{N} K_i \sqrt{\beta_i \beta_N}\sin(\psi_i)\sqrt{\frac{\gamma_i}{\gamma_N}}\left(1 + (N-i)\frac{\tan(\mu/2)}{\tan(\psi_i)}\right)\sin(ks_i)$$

$$g_c(k) \approx \sum_{i=1}^{N} K_i \sqrt{\beta_i \beta_N}\sin(\psi_i)\sqrt{\frac{\gamma_i}{\gamma_N}}\left(1 + (N-i)\frac{\tan(\mu/2)}{\tan(\psi_i)}\right)(\cos(ks_i) - 1) \tag{88}$$

One can see that these functions have resonances at the following wavenumbers

$$kL = \pi j \pm \mu/2 \tag{89}$$

where j is integer. Only four resonances fit into the allowed band $|k| < \pi/L$, the first resonance

$$k_1 L = \mu/2 \tag{90}$$

the second resonance

$$k_2 L = \pi - \mu/2 \tag{91}$$

and also the symmetrical ones for negative k. The values of spectral functions at these resonances can be easily found. Let us split the sum in Eq.(88) in two parts, with odd index $i = 2m-1$ and with even index $i = 2m$ where $m = 1, \ldots, N/2$ (assuming that N is even). The values in the first resonance are then:

$$g_c(k_1) = \sin(N\mu/2)(v_{\mathrm{odd}} + v_{\mathrm{even}}) + \cos(N\mu/2)(w_{\mathrm{odd}} + w_{\mathrm{even}})$$

$$g_s(k_1) = -\cos(N\mu/2)(v_{\mathrm{odd}} + v_{\mathrm{even}}) + \sin(N\mu/2)(w_{\mathrm{odd}} + w_{\mathrm{even}}) \tag{92}$$

the second resonance:

$$g_c(k_2) = \sin(N\mu/2)(-v_{\mathrm{odd}} + v_{\mathrm{even}}) + \cos(N\mu/2)(-w_{\mathrm{odd}} + w_{\mathrm{even}})$$

$$g_s(k_2) = -\cos(N\mu/2)(v_{\mathrm{odd}} - v_{\mathrm{even}}) + \sin(N\mu/2)(w_{\mathrm{odd}} - w_{\mathrm{even}}) \tag{93}$$

Where

$$v_{\text{odd}} \approx \frac{1}{2} K_{\text{odd}} \sqrt{\beta_{\text{odd}} \beta_N} \sum_{m=1}^{N/2} \sqrt{\frac{\gamma_{2m-1}}{\gamma_N}}$$

$$v_{\text{even}} \approx \frac{1}{2} K_{\text{even}} \sqrt{\beta_{\text{even}} \beta_N} \sum_{m=1}^{N/2} \sqrt{\frac{\gamma_{2m}}{\gamma_N}} \tag{94}$$

and

$$w_{\text{odd}} \approx \frac{1}{2} \tan(\mu/2)\ K_{\text{odd}} \sqrt{\beta_{\text{odd}} \beta_N} \sum_{m=1}^{N/2} (N - 2m + 1) \sqrt{\frac{\gamma_{2m-1}}{\gamma_N}}$$

$$w_{\text{even}} \approx \frac{1}{2} \tan(\mu/2)\ K_{\text{even}} \sqrt{\beta_{\text{even}} \beta_N} \sum_{m=1}^{N/2} (N - 2m) \sqrt{\frac{\gamma_{2m}}{\gamma_N}} \tag{95}$$

The resonance values of $G(k)$ and $\mathcal{G}(k)$ are then the following

$$G(k_1) = (v_{\text{odd}} + v_{\text{even}})^2 + (w_{\text{odd}} + w_{\text{even}})^2$$

$$G(k_2) = (v_{\text{odd}} - v_{\text{even}})^2 + (w_{\text{odd}} - w_{\text{even}})^2$$

$$\mathcal{G}(k_1) = \mathcal{G}(k_2) = -v_{\text{odd}}^2 + v_{\text{even}}^2 - w_{\text{odd}}^2 + w_{\text{even}}^2 \tag{96}$$

Behavior in the small vicinity of the peaks can be also found. One can show finally that the peaks can be considered as rectangular ones with full width

$$\Delta k = \frac{2\pi}{NL} \tag{97}$$

If the spectral function are built from coefficients $\hat{d}_i$ defined by (40), the resonance values can be found in similar way. Indeed, one can deduce

$$\hat{d}_i \approx -K_i r_{12}^i + \frac{1}{L} \frac{\Delta\gamma}{\gamma_i} \sqrt{\frac{\gamma_i}{\gamma_N}} \sqrt{\beta_{i+1} \beta_N} \tan(\mu/2) \sin(\mu/2)(N - i) \sin(\psi_i) \tag{98}$$

then one can write

$$v_{\text{odd}} = -K_{\text{odd}} \sqrt{\beta_{\text{odd}} \beta_N} \sum_{m=1}^{N/2} \sqrt{\frac{\gamma_{2m-1}}{\gamma_N}}$$

$$+ \frac{1}{L} \tan(\mu/2) \sin(\mu/2) \sqrt{\beta_{\text{even}} \beta_N} \sum_{m=1}^{N/2} (N - 2m + 1) \frac{\Delta\gamma}{\gamma_{2m-1}} \sqrt{\frac{\gamma_{2m-1}}{\gamma_N}} \tag{99}$$

$$v_{\text{even}} = -K_{\text{even}} \sqrt{\beta_{\text{even}} \beta_N} \sum_{m=1}^{N/2} \sqrt{\frac{\gamma_{2m}}{\gamma_N}}$$

$$+ \frac{1}{L} \tan(\mu/2) \sin(\mu/2) \sqrt{\beta_{\text{odd}} \beta_N} \sum_{m=1}^{N/2} (N - 2m) \frac{\Delta\gamma}{\gamma_{2m}} \sqrt{\frac{\gamma_{2m}}{\gamma_N}} \tag{100}$$

The values in resonances are then given again by (96) with $w_{\text{odd}} = w_{\text{even}} = 0$.

Appendix 2

We saw in the main text that from the spectral point of view an alignment procedure can be considered in terms of evolution of spatial harmonics. For the "one-to-one" techniques the positions of several first quadrupoles of the linac after alignment do not follow exactly the algorithm (21), which describes evolution of harmonics. Nevertheless these details of alignment procedures can also be taken into account within spectral approach.

It is more convenient in this case to start from

$$\eta_x(t) = T_{116}x_{\rm inj}(t) + \sum_{i=1}^{N} d_i\, x_i(t) \tag{101}$$

where the injected angle assumed to be zero. The spectral function are given also by (11,18), but they are composed of parts, which are defined in a slightly different way than in the main text:

$$g_c(k) = \sum_{i=1}^{N} d_i \cos(ks_i) \quad \text{and} \quad g_s(k) = \sum_{i=1}^{N} d_i \sin(ks_i) \tag{102}$$

We start from the "one-to-one" by steering. Let us suppose that $x_{(1-)i}$ is the position of i-th quadrupole just before correction and it corresponds to a single harmonics. In order to find the positions after correction $x_{(1)i}$, one should apply first the algorithm (21) to $x_{(1-)i}$. It will give $x^{\rm alg}_{(1)i}$, which can be composed of two harmonics already. Then the injection position and the positions of the first two quadrupoles should be specified by the following way:

$$x_{\rm inj} = x_{(1)0} = x_{(1-)0} \tag{103}$$

$$x_{(1)1} = x^{\rm alg}_{(1)1} + (x_{(1-)0} - x_{(1-)1})(1 + \frac{2}{LK_1}) \tag{104}$$

$$x_{(1)2} = x^{\rm alg}_{(1)2} + (x_{(1-)0} - x_{(1-)1})\frac{1}{LK_1} \tag{105}$$

The dispersion after correction is then given by

$$\eta_x = T_{116}x_{(1-)0} + \sum_{i=1}^{N} d_i\, x^{\rm alg}_{(1)i}$$

$$+(x_{(1-)0} - x_{(1-)1})\left(d_1(1 + \frac{2}{LK_1}) + \frac{d_2}{LK_1}\right) \tag{106}$$

The rms dispersive error will be finally given by the following expression

$$\langle \eta_x^2(t) \rangle = 2 \int_{k_{\rm min}}^{k_{\rm max}-k_{\rm min}} \left(P(k)G(k) + \mathcal{P}(k)\mathcal{G}(k) + P_{\rm inj}(k)G_{\rm inj}(k) \right) \frac{dk}{2\pi} \tag{107}$$

where the spectral functions $G(k)$ and $\mathcal{G}(k)$ are based on (102) and the additional functions defined as the following:

$$P_{\rm inj}(k) = L(\sigma_{\rm ini}^2 + \sigma_{\rm err}^2) + A\Delta t\left(\frac{1}{k^2} + \frac{1}{k_{\rm max}^2}\right) \tag{108}$$

$$G_{\rm inj}(k) = q_1^2 + q_2^2 + 2(q_1 c + q_2 s) \tag{109}$$

where

$$q_1 = T_{116} + \left(d_1(1 + \frac{2}{LK_1}) + \frac{d_2}{LK_1}\right)(1 - \cos(kL))$$

$$q_2 = \left(d_1(1 + \frac{2}{LK_1}) + \frac{d_2}{LK_1}\right)\sin(kL) \tag{110}$$

and

$$c = g_c(k) + r_2(k)g_c(\tilde{k})$$

$$s = -g_s(k) + r_2(k)g_s(\tilde{k}) \tag{111}$$

Similar consideration can be made for the "one-to-one" by quadrupole moving. If one has one harmonics of the BPM errors $a_i = \cos(ks_i + \phi)$ then the displacements after alignment are given by (48). First, in order to simplify calculations, let us rewrite (48) in the form that will give the same answer for the dispersion, but will not have liner terms:

$$x_i = -\cos(ks_i + \phi) - \frac{KL}{2(1 + \cos(kL))}$$

$$\times\left(\cos(\pi i)\cos(ks_i + \phi) - \cos(\phi) + \frac{T_{126}}{LT_{116}}[\cos(\phi) + \cos(kL + \phi)]\right) \tag{112}$$

One can see now that we can use Eq.(101) with fictitious $x_{\rm inj}$ defined as

$$x_{\rm inj} = \frac{KL}{2(1 + \cos(kL))}\left(a_0(\frac{T_{126}}{LT_{116}} - 1) + a_1\frac{T_{126}}{LT_{116}}\right) \tag{113}$$

The final answer for the dispersive error will be given again by the expression (107), where the additional functions are defined as the following:

$$P_{\rm inj}(k) = L\sigma_{\rm err}^2 \tag{114}$$

The function $G_{\rm inj}(k)$ is given by (109) with the following coefficients

$$q_1 = -r_4(k)(T_{126}/L - T_{116}) - r_4(k)T_{126}/L\cos(kL)$$

$$q_2 = -r_4(k)T_{126}/L\sin(kL) \tag{115}$$

and

$$c = -g_c(k) + r_4(k)g_c(\tilde{k})$$

$$s = -g_s(k) - r_4(k)g_s(\tilde{k}) \tag{116}$$